Charmonium suppression in Pb-Pb collisions

Presented by F.Fleuret[9], for the NA50 Collaboration

M.C. ABREU[6a], B. ALESSANDRO[11b], C. ALEXA[2], J. ASTRUC[8], C. BAGLIN[1], A. BALDIT[4], M. BEDJIDIAN[12], F. BELLAICHE[12], S. BEOLÈ[11b], V. BOLDEA[2], G. BONAZZOLA[11b], P. BORDALO[6h], A. BORHANI[9], A. BUSSIÈRE[1], V. CAPONY[1], J. CASTOR[4], T. CHAMBON[4], B. CHAURAND[9], I. CHEVROT[4], B. CHEYNIS[12], E. CHIAVASSA[11b], C. CICALÓ[3], S. CONSTANTINESCU[2], J. CRUZ[6], W. DABROWSKI[11b], A. DE FALCO[3], G. DELLACASA[11d], N. DE MARCO[11b], A. DEVAUX[4], S. DITA[2], O. DRAPIER[12], B. ESPAGNON[4], J. FARGEIX[4], F. FLEURET[9], P. FORCE[4], M. GALLIO[11b], L. GATIGNON[5], Y.K. GAVRILOV[7], C. GERSCHEL[8], P. GIUBELLINO[11b], M.B. GOLUBEVA[7], M. GONIN[9], P. GORODETZKY[10], J.Y. GROSSIORD[12], P. GUAITA[11b,e], F.F. GUBER[7], A. GUICHARD[12], R. HAROUTUNIAN[12], M. IDZIK[11b], D. JOUAN[8], T.L. KARAVITCHEVA[7], L. KLUBERG[9], A.B. KUREPIN[7], G. LANDAUD[4], Y. LE BORNEC[8], C. LOURENÇO[5], L. LUQUIN[4], P. MACCIOTTA[3], A. MARZARI-CHIESA[11b], M. MASERA[11b], A. MASONI[3], S. MOURGUES[4], A. MUSSO[11b], F. OHLSSON-MALEK[12], P. PETIAU[9], A. PICCOTTI[11b], J.R. PIZZI[12], W.L. PRADO DA SILVA[11b,f], G. PUDDU[3], C. QUINTANS[6], C. RACCA[10], L. RAMELLO[11c], S. RAMOS[6h], P. RATO-MENDES[11b], L. RICCATI[11b], A. ROMANA[9], S. SARTORI[11], P. SATURNINI[4], E. SCOMPARIN[11b,g], S. SERCI[3], R. SHAHOYAN[5], S. SILVA[6], P. SONDEREGGER[5h], X. TARRAGO[8], P. TEMNIKOV[3], N.S. TOPILSKAYA[7], G. USAI[3], C. VALE[6], E. VERCELLIN[11b], and N. WILLIS[8].

[1] *Laboratoire de Physique des Particules (LAPP), IN2P3-CNRS, Annecy-le-Vieux, France;*
[2] *Institute of Atomic Physics (IFA), Bucharest, Romania;*
[3] *Università di Cagliari/INFN, Cagliari, Italy;*
[4] *Laboratoire de Physique Corpusculaire, Université Blaise Pascal et IN2P3-CNRS, Clermont-Ferrand, France;*
[5] *CERN, Geneva, Switzerland;*
[6] *Laboratório de Instrumentação e Fisica Experimental de Partículas (LIP), Lisbon, Portugal;*
[7] *Institute for Nuclear Research (INR), Moscow, Russia;*
[8] *Institut de Physique Nucléaire, Université Paris-Sud et IN2P3-CNRS, Orsay, France;*
[9] *Ecole Polytechnique et IN2P3-CNRS, Laboratoire de Physique Nucléaire des Hautes Energies, Palaiseau, France;*
[10] *Centre de Recherches Nucléaires, Université Louis Pasteur et IN2P3-CNRS, Strasbourg, France;*
[11] *Università di Torino e INFN, Turin, Italy ;*
[12] *Institut de Physique Nucléaire de Lyon, Université Claude Bernard et IN2P3-CNRS , Villeurbanne, France.*

[a] *Also at FCUL, Universidade de Lisboa, Lisbon, Portugal;* [b] *Dipartimento di Fisica Sperimentale;* [c] *Dipartimento di Scienze e Tecnologie Avanzate;* [d] *II Facoltà di Scienze, Alessandria;* [e] *Now at Dipartimento di Fisica, Università di Padova, Padua, Italy;* [f] *Now at UERJ, Rio de Janeiro, Brazil;* [g] *Now at CERN, Geneva, Switzerland;* [h] *Also at IST, Universidade Técnica de Lisboa, Lisbon, Portugal.*

Abstract

Results on J/ψ, ψ' and Drell-Yan production in Pb-Pb reactions at 158 GeV/c per nucleon are reported and compared with previous results obtained by the NA38 and NA51 experiments. The ratios $B_{\mu\mu}\sigma_{J/\psi}/\sigma_{Drell-Yan}$ and $B'_{\mu\mu}\sigma_{\psi'}/\sigma_{Drell-Yan}$ are given as a function of the centrality of the collision.

Introduction

The NA50 experiment measures vector mesons production via their decays into muon pairs in Pb-Pb interactions at 158 GeV/c per nucleon. The main goal is the study of charmonia suppression as an evidence for the formation of the quark-gluon plasma [1]. Starting in 1986 at the CERN SPS, J/ψ and ψ' suppressions have been first studied by the NA38 collaboration using proton, oxygen and sulfur induced reactions which are used as a reference for the study of Pb-Pb interactions.

1 Experimental conditions

The NA50 detector is an upgraded version of the NA38 apparatus. It is mainly composed of a dimuon spectrometer, a segmented active target, an electromagnetic calorimeter and a very forward hadronic calorimeter ("Zero Degree Calorimeter") to provide two independent estimates of the centrality. Appropriate beam counters are used to measure the incident flux.

The *dimuon spectrometer* uses basically the same components as the spectrometer of the NA38 experiment [2]. It covers the pseudo-rapidity interval $2.8 < \eta < 4.0$ and the mass resolution obtained for the J/ψ is 3.1 % .

The *target* is made of 7 Pb subtargets of 1 mm thick leading to a total of 17.5 % interaction lenght. Each subtarget is followed downstream by two associated quartz blades located off the beam axis and used to identify the primary vertex and reject events with secondary reinteractions.

The *electromagnetic calorimeter* measures the neutral transverse energy produced in the interaction in the pseudo-rapidity range $1.1 < \eta < 2.3$. This measurement provides the impact parameter of the collision. It exhibits a good linear correlation with the information given by the ZDC which measures the energy deposited by the spectator fragments of the interacting projectile.

The data presented here were taken during 5 weeks in 1995 with an incident flux of $3.5\ 10^7$ ions/burst leading to an average of 1000 dimuon triggers/burst. During this run, a sample of roughly 60 million triggers was recorded.

2 Event selection and analysis

Several cuts were applied to the data. Events are selected for the final analysis if :

- only one incident ion is detected within the 20 ns gate opened by the trigger.
- the subtarget of the primary interaction is identified by the target algorithm and if the projectile spectator does not reinteract in any following subtarget.
- only one incident ion is detected by the ZDC.

The tracking algorithm requires two muon tracks in the acceptance of the spectrometer which defines the kinematical domain:

$$0. < y_{cm} < 1. \qquad \Longleftrightarrow \qquad 2.92 < y_{lab} < 3.92$$

$$-0.5 < \cos\theta_{CS} < 0.5$$

where y is the dimuon rapidity and θ_{CS} the polar angle of one of the muons in the Collins-Soper reference frame.

Figure 1 shows the invariant mass spectrum of the opposite sign muon pairs for masses above 2.0 GeV/c^2. The contributing processes are J/ψ, ψ', Drell-Yan, $D\bar{D}$ pairs and

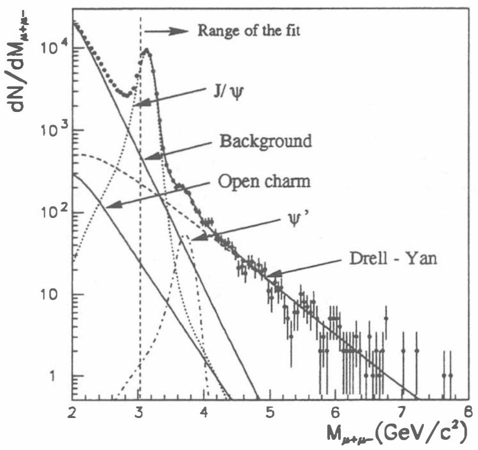

Figure 1: *Opposite sign mass spectrum for Pb-Pb collisions.*

the background of π and K meson decays. The background estimation is based on the measured like sign muon pairs, using the relation:

$$N^{bg} = 2 \times \sqrt{N^{++} \times N^{--}}$$

In order to measure the number of J/ψ, ψ' and Drell-Yan events, the invariant mass spectrum is fitted for masses above 3.05 GeV/c^2, using the maximum likelihood method, with a superposition of all the processes:

$$\frac{dN^{+-}}{dM_{\mu\mu}} = \frac{dN^{J/\psi}}{dM_{\mu\mu}} + \frac{dN^{\psi'}}{dM_{\mu\mu}} + \frac{dN^{DY}}{dM_{\mu\mu}} + \frac{dN^{D\bar{D}}}{dM_{\mu\mu}} + \frac{dN^{bg}}{dM_{\mu\mu}}$$

where the ratio of the $D\bar{D}$ to Drell-Yan events is fixed from the study of p-W data [3].

The acceptance of the apparatus and the shapes of J/ψ, ψ', Drell-Yan and $D\bar{D}$ contributions are determined by Monte-Carlo simulations.

3 Cross sections for J/ψ and Drell-Yan

Absolute cross-sections are calculated taking into account detector efficiencies, selection cut losses and acceptances which lead to a systematic error of 7 %. They amount to :

$$B_{\mu\mu}\sigma_{J/\psi} = 21.9 \pm 0.2 \pm 1.6 \ \mu b$$

$$\sigma_{Drell-Yan} = 1.49 \pm 0.02 \pm 0.11 \ \mu b \qquad (2.9 < M_{\mu\mu} < 8.0 \text{ GeV}/c^2)$$

The Drell-Yan cross section value in Pb-Pb collisions has been compared with previous results obtained in p-A and S-U collisions. To account for differences in the kinematical domains and beam energies, the comparison is made using the so-called "K factor" which is the ratio between the measured cross-section value and the lower order theoretical cross-section calculated from the GRV-LO [4] set of parton distribution functions. The results are presented in figure 2 (left) as a function of $A \times B$ (the product of the projectile and target atomic mass numbers) showing a good Pb-Pb agreement with lighter projectile results and with the Drell-Yan theoretical calculations which are proportionnal to $A \times B$.

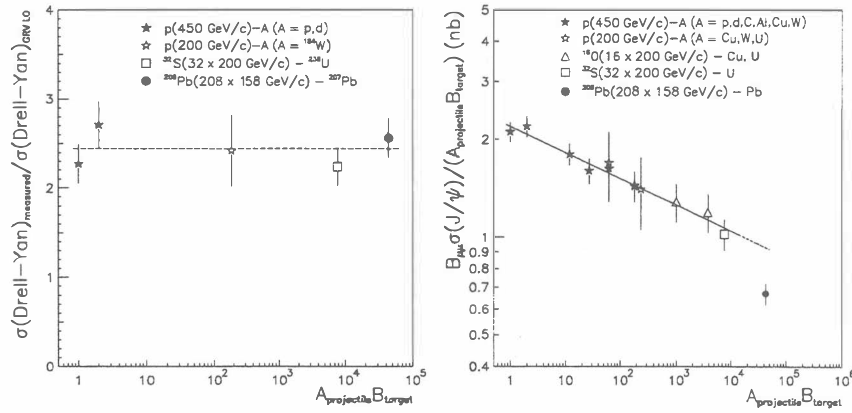

Figure 2: *Left: the Drell-Yan K factor as a function of* $A_{projectile}B_{target}$. *Right: the J/ψ cross-section divided by* $A_{projectile}B_{target}$ *as a function of* $A_{projectile}B_{target}$.

Figure 2 (right) shows $B_{\mu\mu}\sigma_{J/\psi}$ divided by $A \times B$ (the cross-section per nucleon-nucleon collision) as a function of $A \times B$ for several systems. All the data are rescaled to the same kinematical domain ($0. < y_{cm} < 1.$) and to the same beam energy (200 GeV/c). The Pb-Pb result is rescaled to 200 GeV/c using the Schuler parametrization [5].
Except for the Pb point, all the data decrease with $A \times B$ as the power law function $(A \times B)^{\alpha}$ with $\alpha = 0.920 \pm 0.015$ in good agreement with previous measurements [6]. For Pb-Pb collisions, the J/ψ cross-section is a factor 0.74 ± 0.06 smaller than the expected value obtained with the power law, showing an additionnal J/ψ suppression.

4 Cross sections as a function of centrality

In the study of charmonia production as a function of centrality, we have used the variable $\bar{L}$, the average path length of the resonant (or pre-resonant) state through nuclear matter [7]. $\bar{L}$ is related to the impact parameter b and is calculated within a geometrical model using the standard Woods-Saxon nuclear density distributions. As already mentionned, the impact parameter is correlated with the measured transverse energy E_T. Thus, selecting the events in transverse energy bins is equivalent to select events in b or $\bar{L}$ bins. Figure 3 (left) shows the relation between $\bar{L}$ and E_T. In this analysis, the data

E_T bin (GeV)	$< E_T >$ (GeV)	$\bar{L}$
5 - 45	34	6.94 ± 0.49
45 - 70	58	7.98 ± 0.36
70 - 105	88	8.86 ± 0.30
105 - 135	120	9.43 ± 0.17
135 - 175	147	9.71 ± 0.15

Table 1: E_T *bins, related mean values* $< E_T >$ *and corresponding* $\bar{L}$.

are divided in 5 transverse energy bins. The corresponding values of E_T and $\bar{L}$ are given

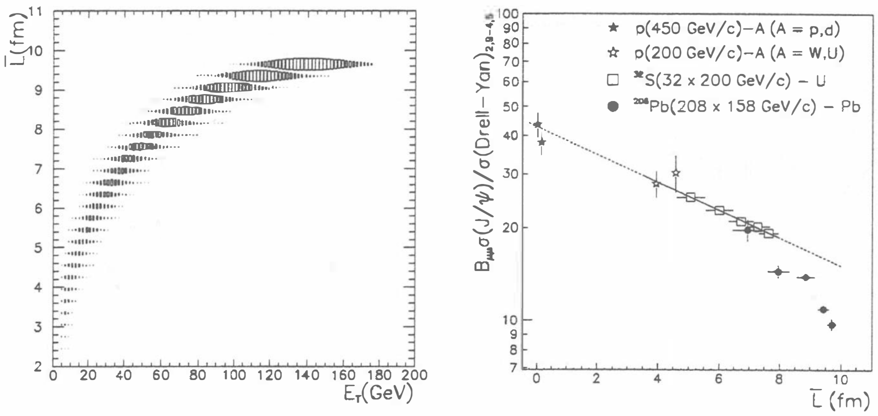

Figure 3: *Left: $\bar{L}$ as a function of the transverse energy E_T. Right: $B_{\mu\mu}\sigma_{J/\psi}/\sigma_{Drell-Yan}$ as a function of $\bar{L}$; the solid line corresponds to the absorption model with $\sigma_{abs} = 6.2$ mb.*

in table 1. Moreover, as the Drell-Yan cross-section is proportional to the product $A \times B$, studying $B_{\mu\mu}\sigma_{J/\psi}/\sigma_{Drell-Yan}$ is equivalent to study $B_{\mu\mu}\sigma_{J/\psi}/A \times B$ with the avantage of cancelling all systematic errors due to beam flux uncertainties and detector efficiencies.

Figure 3 (right) displays the ratio $B_{\mu\mu}\sigma_{J/\psi}/\sigma_{Drell-Yan}$ for the 5 centrality bins defined in table 1. Data are rescaled to 200 GeV/c and compared with previous measurements from NA38 (p-W, p-U and S-U) and NA51 (p-p, p-d).
Except for the Pb points, all the data decrease exponentially with $\bar{L}$. This behaviour can be interpreted as the result of the pre-resonant $c\bar{c}g$ state absorption in nuclear matter [8]. Thus, $B_{\mu\mu}\sigma_{J/\psi}$ can be written as $\sigma_0 \exp(-\rho_0 \bar{L}\sigma_{abs})$ where $\rho_0 = 0.17$ fm^{-3} is the standard nuclear density and σ_{abs} is the absorption cross-section. A fit to the data leads to $\sigma_{abs} = 6.2 \pm 0.7$ mb.
Comparing to this absorption model, the integrated Pb-Pb $B_{\mu\mu}\sigma_{J/\psi}/\sigma_{Drell-Yan}$ value shows an overall suppression by a factor 0.71 ± 0.03 which is more than 9 standard deviations below the expected value. The study in 5 E_T bins shows a strong dependence of this effect with the centrality of the collision. The measured value is a factor 0.95 ± 0.09 below the expected value for the most peripheral reactions (first E_T bin), and a factor 0.62 ± 0.04 for the most central Pb-Pb collisions.

5 ψ' production

In figure 4 (left) we plot the cross-section ratios $B'_{\mu\mu}\sigma_{\psi'}/B_{\mu\mu}\sigma_{J/\psi}$ as a function of $A \times B$ for several systems including p-A, S-U and Pb-Pb collisions without any rescaling correction to take into account the various beam energies (as already pointed out [9] this ratio is independent of energy).
For proton induced reactions, $B'_{\mu\mu}\sigma_{\psi'}/B_{\mu\mu}\sigma_{J/\psi}$ is independent of the target mass, the average value beeing $(1.75 \pm 0.02)\%$. This behaviour can be interpreted as the absorption of the pre-resonant $c\bar{c}g$ state in nuclear matter which does not depend on the final charmonium state.
In ion induced reactions, ψ' is more suppressed than J/ψ as compared to p-A systems, without significant change between S-U ($B'_{\mu\mu}\sigma_{\psi'}/B_{\mu\mu}\sigma_{J/\psi} = (0.76 \pm 0.06)\%$) and Pb-Pb

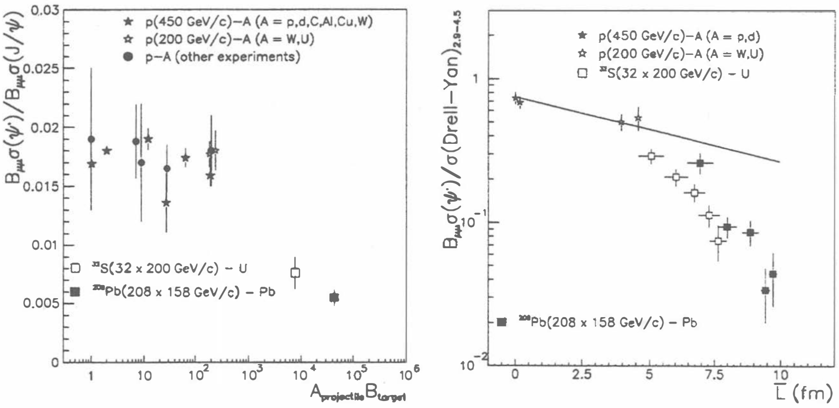

Figure 4: *Left:* $B'_{\mu\mu}\sigma_{\psi'}/B_{\mu\mu}\sigma_{J/\psi}$ *as a function of* $A \times B$. *Right:* $B'_{\mu\mu}\sigma_{\psi'}/\sigma_{Drell-Yan}$ *as a function of* $\bar{L}$*; the solid line corresponds to the absorption model with* $\sigma_{abs} = 6.2$ *mb.*

($B'_{\mu\mu}\sigma_{\psi'}/B_{\mu\mu}\sigma_{J/\psi} = (0.55 \pm 0.07)\%$) collisions. In fact, because of the anomalous J/ψ suppression in Pb-Pb, ψ' is more suppressed in Pb-Pb as compared with S-U collisions. Figure 4 (right) displays the $B'_{\mu\mu}\sigma_{\psi'}/\sigma_{Drell-Yan}$ ratio as a function of $\bar{L}$, showing an increasing suppression of ψ' from S-U to Pb-Pb collisions. Hovewer, as opposed with J/ψ suppression, the ψ' suppression pattern is similar in Pb-Pb and S-U interactions.

Conclusion

J/ψ and ψ' productions have been studied in Pb-Pb collisions at 158 GeV/c per nucleon. An anomalous J/ψ suppression in Pb-Pb is observed as compared with the absorption model based on p-A and S-U results. Looking at ψ' production, a stronger suppression than expected by the absorption model is observed in S-U and Pb-Pb collisions with a similar suppression pattern for both reactions.

References

[1] T. Matsui and H. Satz, Phys. Lett. B 178 (1986) 416.

[2] C. Baglin *et al.*, Phys. Lett. B 220 (1989) 471.

[3] E. Scomparin *et al.*, Nucl. Phys. A 610 (1996) 331c.

[4] M. Glück *et al.*, Phys. Lett. B 306 (1993) 391.

[5] G. A. Schuler, CERN-TH.7170/94.

[6] J. Badier *et al.*, Z. Phys. 20 (1983) 101;
D. M. Alde *et al.*, Phys. Rev. Lett. 66 (1991) 133;
L. Antoniazzi *et al.*, Phys. Rev. D 46 (1992) 4828;
M. S. Kowitt *et al.*, Phys. Rev. Lett. 72 (1994) 1318.

[7] C. Gerschel and J. Hüfner, Z. Phys. C56 (1992) 71.

[8] D. Kharzeev and H. Satz, Phys. Lett. B366 (1996) 316.

[9] C. Lourenço, Nucl. Phys. A610 (1996) 552c.